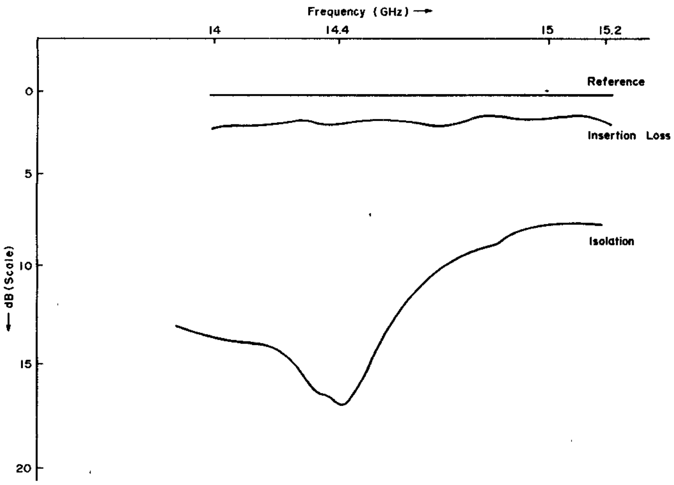

Fig. 5. *Ku*-band MILIC isolator optimized for high isolation.

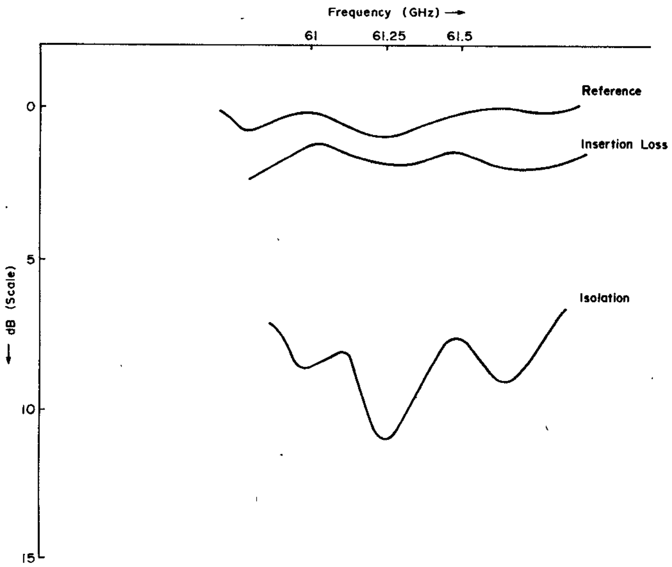

Fig. 6. *V*-band MILIC isolator.

The dimensions of magnetic pole pieces have to retain a certain form factor to supply the high biasing field. Magnet materials having high-energy product diagram (rare earth type) were mainly used.

C. Experimental Results

To verify the design concept of the edge-loaded MILIC isolator, a few devices were fabricated and tested. The initial experimental effort was carried out in *Ku* band. A figure of merit of 10 is feasible for this type of device. Table I lists the electrical and mechanical characteristics of the *Ku*-band MILIC device. Performance characteristics are shown in Fig. 5.

A MILIC isolator at *V* band was also fabricated using a configuration similar to the *Ku*-band device. The performance characteristics are shown in Fig. 6. A figure of merit of about 10 was also achieved for this band. Table II lists the electrical and mechanical characteristics of the *V*-band MILIC device.

TABLE II
CHARACTERISTICS OF *V*-BAND DEVICE

Center Frequency:	61.25 GHz
Isolation:	11 dB
Insertion Loss:	1 dB
Bandwidth:	≈ 250 MHz between 8-dB points
Size of Composite Guide:	0.8 in. × 0.040 in. × 0.028 in. (ceramic)
	0.8 in. × 0.040 in. × 0.018 in. (ferrite)
Ferrite Material:	Nickel-Ferrite, Trans Tech TT2-111
Tuning Slab:	0.8 in. × 0.040 in. × 0.02 in.
Biasing Field in Device Gap:	4400 gauss.

IV. CONCLUSIONS

In this short paper, theoretical design considerations and experimental results for a ferrite isolator in the MILIC technology have been presented. The function of the device is based on the utilization of the fringe-field effect. This device constructed at 14.4 and 61.25 GHz showed an isolation of 17.5 and 11 dB, respectively. The corresponding insertion losses were 1.8 and 1.0 dB.

The concepts discussed in this short paper can lead to evolution of various other types of ferrite devices. For example, a three-port circulator can be formed by laying the edge-loaded isolator configuration in a δ-junction geometry with access ports. Among other components, a nonreciprocal phase shifter and a differential-phase-shift circulator in the MILIC geometry are also conceivable. With various adaptations of these forms, several ferrite device applications can be realized. It is estimated that a ferrite device using sandwich configuration will have a higher figure of merit compared to the edge-loaded configuration. Ferrite devices in MILIC geometry have the advantage of being compact and of low cost compared to the ferrite devices in conventional structures.

REFERENCES

[1] "Image line integrated circuit for system applications at millimeter wavelengths," Final Report, Contract DAAB07-73-C-0217 to IIT Research Institute, Chicago, U.S. Army Electronics Command Report ECOM-73-0217-F, July 1974.
[2] R. M. Knox and P. P. Toulios, "Integrated circuits for the millimeter through optical frequency range," Proc. Symposium on Submillimeter Waves, Polytechnic Institute of Brooklyn, N.Y., March 31–April 2, 1970.
[3] J. E. Kietzer, A. R. Kaurs, and B. T. Levin, "A *V*-band communication transmitter and receiver system using dielectric waveguide integrated circuits," this issue, pp. 797–803.
[4] A. R. Kaurs, "A tunable bandpass ring filter for rectangular dielectric waveguide integrated circuits," this issue, pp. 875–876.
[5] Y. Shiau, "Dielectric rod antennas for millimeter-wave integrated circuits," this issue, pp. 869–872.
[6] "Hybrid millimeter wave integrated circuits," Final Rep., Contract DAAB07-74-C-0577 to IIT Res. Inst., Chicago, IL, U.S. Army Electronics Command Rep. ECOM-74-0577-F, Oct. 1975.

The Fabrication of Dielectric Image Lines Using Casting Resins and the Properties of the Lines in the Millimeter-Wave Range

KLAUS SOLBACH

Abstract—**Experiments with dielectric image lines fabricated of casting resins are described, and the properties of the electromagnetic fields and the phase coefficients of the waves in the millimeter-wave range (26–40 GHz) are discussed. As an example, a ring resonator and the measurement of its insertion loss is presented.**

Manuscript received February 11, 1976; revised May 6, 1976.
The author is with the Lehrstuhl für Allgemeine und Theoretische Elektrotechnik, University of Duisburg, West Germany.

I. Introduction

Dielectric image lines and their applications for millimeter-wave integrated circuits have been proposed during the last years [1]–[7]. As far as the author knows two fabrication methods for building dielectric image lines have been discussed in the literature: 1) fabrication of the lines from ceramic disks by mechanical treatment [7], and 2) fabrication with the semi-conducting materials silicon and gallium arsenide [6].

If the dielectric lines and their properties are to be investigated systematically, a number of lines with different geometrical dimensions must be produced in the laboratory. For example, it should be possible to make lines of different lengths but of exactly the same cross section. Therefore, casting resins and thermoplastics were used in a dielectric casting technique to pour the image lines into molds.

II. Dielectric Image Lines of Paraffin Wax and Stycast Resin

Two materials have been used to cast dielectric image lines: 1) paraffin wax, $\varepsilon_r = 2.22$, $\tan \delta = 6 \cdot 10^{-4}$, 2) Stycast resin 35 DA, $\varepsilon_r = 3.4$, $\tan \delta = 2.7\ 10^{-3}$, delivered by Emerson and Cuming. Paraffin wax is a thermoplastic material of small strength and a low melting point (50°C). Because of the low melting point the material is well suited for experiments in the laboratory. The lines can be produced very easily. On the other hand, because of the temperature sensibility and the low mechanical strength, the lines cannot be used to fabricate commercial circuits. Stycast 35 DA is a ceramic-filled resin, which cross-links at moderately elevated temperatures to polystyrene. It must be cured for more than 12 h and therefore is not as easy to handle as paraffin wax; but, it is greater in strength, and, hence, the lines and circuits produced could meet the mechanical requirements for industrial applications. Resins that offer a range of dielectric constants from 3 to 25 such as 3M's Custom High-K 707 castable dielectric, promise even better properties than the Stycast resin. Other thermoplastics like polystyren and polyethylene, which have properties similar to those of paraffin wax but have a higher melting point, can be used also.

Both of the materials under investigation have a small dielectric constant. This is a disadvantage if high-Q circuits are to be produced. But it is an advantage, if the fundamental field distributions of the lines are examined experimentally since a great part of the electromagnetic field is outside the dielectric medium in the air region. The loss tangent of the Stycast material is somewhat high as compared with Al_2O_3 ceramics, and the lines produced with this material will not have a high Q factor, which is a disadvantage if resonators or filters of small bandwidths are to be built.

As the fabrication technique for the lines and circuits is similar to the well-known die casting process, it is applicable for mass production. The liquid material is injected under high pressure into the molds. If thermoplastics such as paraffin wax or polystyrene are used, pressure must be applied during the cooling period to gain a shrinkage compensation. The molds used in these experiments were aluminium, in which the contour of the image line was milled with a heavy machine tool. The mold was screwed to a ground plane and the casting compounds were injected into the cavities so that the mold could be removed after the material cooled.

In Fig. 1(a), as an example, the mold of a ring resonator coupled to a straight line as well as the produced circuit are shown. The ring resonators were used to study the radiation characteristics of curved dielectric image lines. For this purpose resonators with different radii were built and the dependence of Q factors on curvature was measured. Fig. 1(b) shows the measured insertion loss of the circuit, from which the resonance frequencies and the Q factors of the resonator can be calculated.

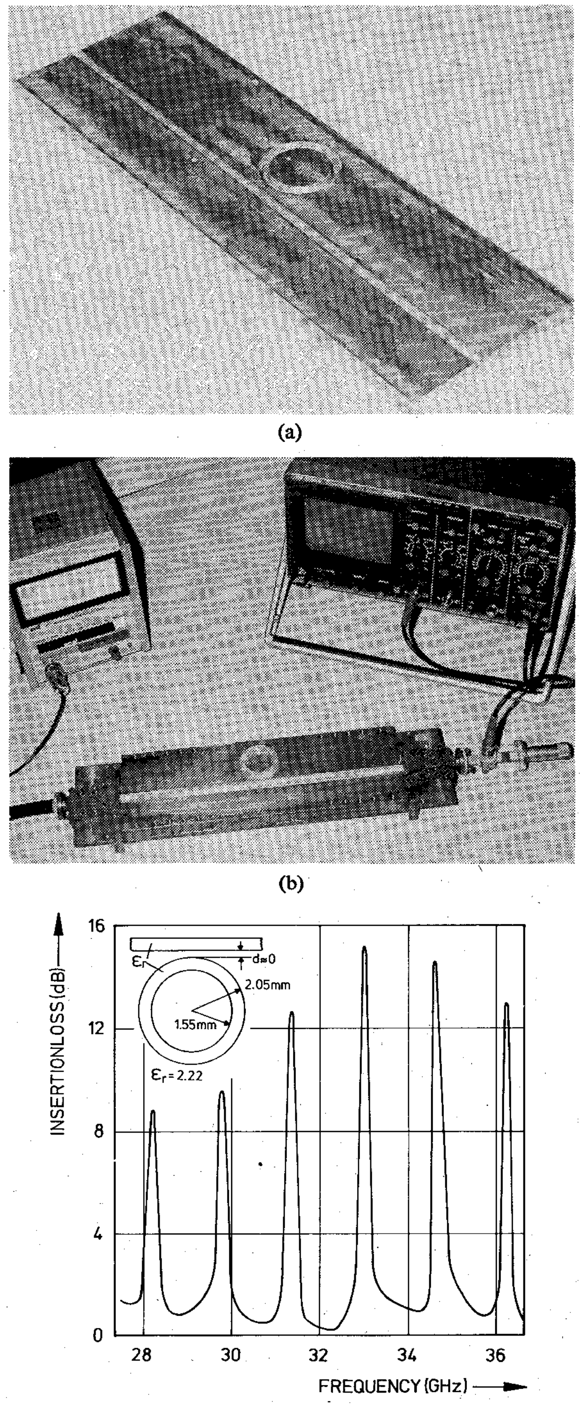

Fig. 1 (a) Mold for a dielectric image line ring resonator. (b) The produced resonator. (c) The measured insertion loss of the circuit.

III. Measurements on Dielectric Image Lines

The phase constant of single lines and two coupled lines have been measured using line resonators. The resonators were built out of dielectric image lines which are shorted at both ends. They are coupled to a metal waveguide by a coupling hole in the ground plane. Using a field probe, the field distribution of the oscillating resonators was scanned. The field probe was con-

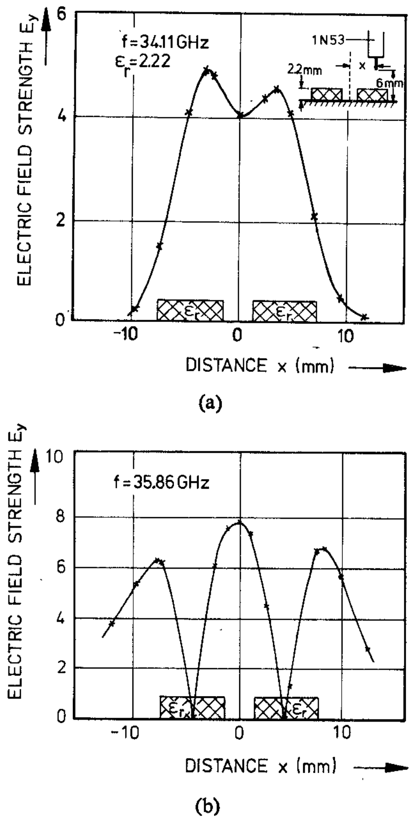

Fig. 2. Measured field distribution in the cross section of two coupled dielectric image lines. (a) EH_{11} ($E_{11}{}^{y}$) even mode. (b) EH_{21} ($E_{21}{}^{y}$) even mode.

structed using a 1N53 diode. The coaxial inner conductor couples to the electric field of the lines since the outer conductor is partly removed. This field probe is much more sensitive than those which use a metal waveguide with a coupling probe [8]. Since the probe is relatively small, the disturbance of the electromagnetic field is tolerable. From the measured maxima of the electric field strength along the line and in the cross section, the guide wavelength and mode of the wave can be detected.

In Fig. 2 the field distribution of the electric field for (a) the $E_{11}{}^{y}$ even mode and (b) the $E_{21}{}^{y}$ even mode on two coupled image lines of paraffin wax at 34 GHz are shown. The field can be detected very accurately, which can be seen especially from the detection of the zeros of the $E_{21}{}^{y}$ mode.

The even mode can be detected symmetrically. The odd mode normally is not as symmetrical as the even mode if the line is excited by only one coupling probe. The field distribution of the odd mode differs from that of the even mode by a zero between the lines, so that both modes can be distinguished very easily.

In Fig. 3 the decay of the electromagnetic field in two dimensions near the edges of a single image line is drawn. As can be seen, the fields decay like an exponential function. The decay coefficients depend on the frequency.

An approximate calculation for the phase constant of the waves on a dielectric image line is described in [1] and [2]. In both papers it has been assumed that the electromagnetic field in the region $x > w, y > h$ ($2 \cdot w =$ width of one dielectric image line, $h =$ height of the line) is zero. As can be seen from Fig. 3, this assumption is verified very well if the frequency is so high that the electromagnetic wave is well guided by the image line, i.e., λ_0/λ_g is at least greater than 1.1.

Corresponding to this result, the measured phase constants of the image lines are in good agreement with the predicted values

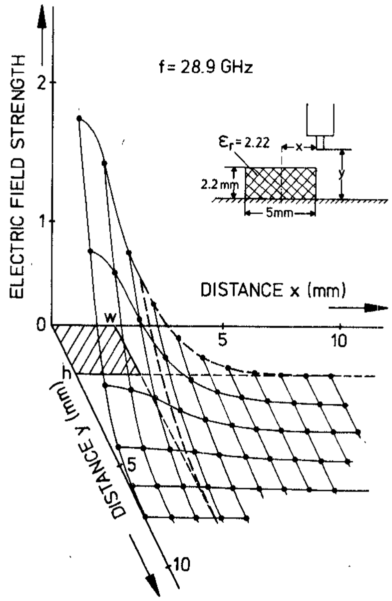

Fig. 3. Measured decay of the electromagnetic field of a single dielectric image line near the edges of the line ($\lambda_0/\lambda_g = 1.12$).

of Toulios and Knox's theory [1] as has been shown in [9]. The wavelengths of the even mode as well as those of the odd mode agree well with the theory as long as the ratio λ_0/λ_g is greater than 1.1.

References

[1] R. M. Knox and P. P. Toulios, "Integrated circuits for the millimeter through optical frequency range," in *Proc. Symp. Submillimeter-Waves.* Brooklyn, NY: Polytechnic Press of Polytechnic Institute of Brooklyn, 1970, pp. 497–516.
[2] E. A. J. Marcatili, "Dielectric rectangular waveguide and directional coupler for integrated optics," *Bell Syst. Tech. J.*, vol. 48, pp. 2071–2102, Sept. 1969.
[3] P. P. Toulios and R. M. Knox, "Rectangular dielectric image lines for millimeter integrated circuits," in *Western Electronic Show and Convention*, pp. 1–10, August 25–29, 1970.
[4] R. M. Knox, P. P. Toulios, and J. Q. Howell, "Radiation losses in curved dielectric image waveguides of rectangular cross section," in *Digest IEEE Intern. Microwave Symp.*, pp. 25–27, 1973.
[5] J. E. Goell, "A circular-harmonic computer analysis of rectangular dielectric waveguides," *Bell. Syst. Tech. J.*, vol. 48, pp. 2133–2160, Sept. 1969.
[6] M. M. Chrepta and H. Jacobs, "Millimeter-wave integrated circuits," *Digest IEEE Microwave Symp.*, p. 198, 1974.
[7] ——, "Millimeter-wave integrated circuits cost less using dielectric waveguides," *Microwave J.*, vol. 17, pp. 45–47, Nov. 1974.
[8] J. F. Heitmann, "Theory and fabrication of dielectric image lines and measurements in the frequency range from 62.5 to 40 GHz," *Nachrichtentech. Z.* (Germany), vol. 28, pp. 279–284, August 1975.
[9] K. Solbach, "Integrierte Millimeterwellenschaltungen," Research Rep. DFG (Deutsche Forschungsgemeinschaft), Wo 137/2, 1976.

22-GHz Measurements of Dielectric Constants and Loss Tangents of Castable Dielectrics at Room and Cryogenic Temperatures

ROBERT W. HAAS, MEMBER, IEEE, AND PETER ZIMMERMANN

***Abstract*—The dielectric constants and loss tangents of a number of castable dielectrics such as different epoxies were measured at 22 GHz at both room temperature and 77 K using a resonant cavity technique. It was found that these high-frequency values differ significantly from published low-frequency values, and that the losses decrease dramatically at cryogenic temperatures.**

Manuscript received February 2, 1976; revised May 12, 1976.
The authors are with the Max-Planck-Institute for Radio Astronomy, 5300 Bonn 1, Germany.